SECURITY CLASSIFICATION OF THIS PAGE

1043

AD-A278 475

1a. REPORT SECURITY CLASSIFICATION: Unclassified

2a. SECURITY CLASSIFICATION AUTHORITY

2b. DECLASSIFICATION/DOWNGRADING SCHEDULE

LITY OF REPORT

Approved for public release; distribution unlimited.

4. PERFORMING ORGANIZATION REPORT NUMBER(S)

5. MONITORING ORGANIZATION REPORT NUMBER(S): AFOSR-TR- 94 0145

6a. NAME OF PERFORMING ORGANIZATION: Department of Chemistry University of Denver

6b. OFFICE SYMBOL (If applicable)

7a. NAME OF MONITORING ORGANIZATION: AFOSR/NC

6c. ADDRESS (City, State and ZIP Code): Denver, Colorado 80208

7b. ADDRESS (City, State and ZIP Code): 110 Duncan Ave Bolling AFB DC 20332-0001

8a. NAME OF FUNDING/SPONSORING ORGANIZATION: AFOSR/NC

8b. OFFICE SYMBOL (If applicable): NC

9. PROCUREMENT INSTRUMENT IDENTIFICATION NUMBER: F49620-92-J-0270

8c. ADDRESS (City, State and ZIP Code): 110 Duncan Avenue, Suite B115 Bolling AFB, DC 20332-0001

10. SOURCE OF FUNDING NOS.

PROGRAM ELEMENT NO.	PROJECT NO.	TASK NO.	WORK UNIT NO.
6321BC	1601	08	

11. TITLE (Include Security Classification): Reactions and Spectroscopy of Excited Nitrenes

12. PERSONAL AUTHOR(S): Robert D. Coombe

13a. TYPE OF REPORT	13b. TIME COVERED	14. DATE OF REPORT (Yr., Mo., Day)	15. PAGE COUNT
Final Report	FROM 1-May-92 TO 31-Oct-93	28 January 94	40

16. SUPPLEMENTARY NOTATION

17. COSATI CODES			18. SUBJECT TERMS (Continue on reverse if necessary and identify by block number)
FIELD	GROUP	SUB. GR.	

19. ABSTRACT (Continue on reverse if necessary and identify by block number)

This report describes the results of an 18 month research program in which reactions and energy transfer processes involving excited $NCl(a^1\Delta)$ were investigated. The work included three projects. In the first of these, high densities ($>10^{15}cm^{-3}$) of $NCl(a^1\Delta)$ were produced by photodissociation of ClN_3, and excited $I(5^2P_{1/2})$ atoms were generated by a subsequent energy transfer process. The data suggest that a population inversion on the $I(5^2P_{1/2})$ - $I(5^2P_{3/2})$ transition was achieved, but the inversion density was insufficient to reach laser theshold in the optical cavity employed. In the second project, rate constants for collisional quenching of $NCl(a^1\Delta)$ by a number of atoms and diatomic molecules were measured.. In the third project, the production of $NCl(a^1\Delta)$ by the H + NCl_2 reaction was investigated in a continuous transverse-flow reactor, at high reagent densities.

20. DISTRIBUTION/AVAILABILITY OF ABSTRACT

UNCLASSIFIED/UNLIMITED ☒ SAME AS RPT. ☐ OTIC USERS ☐

21. ABSTRACT SECURITY CLASSIFICATION: Unclassified

22a. NAME OF RESPONSIBLE INDIVIDUAL	22b. TELEPHONE NUMBER (Include Area Code)	22c. OFFICE SYMBOL
~~Robert D. Coombe~~ Dr Michael Berman	~~(303) 871-2436~~ 202-767-4963	NC

DD FORM 1473, 83 APR EDITION OF 1 JAN 73 IS OBSOLETE.

SECURITY CLASSIFICATION OF THIS PAGE

INTRODUCTION

The electronically excited singlet states of halogen nitrenes have been of interest for a number of years because of their utility as energy storage agents in chemical lasers. In particular, potential lasers based on energy transfer from the $a^1\Delta$ states of NF, NCl, and NBr have been investigated by a number of groups.[1] Within the last two years, these efforts have come to fruition with the demonstration by Benard and co-workers[2] of lasing on the $A \rightarrow X$ transition of BiF, pumped by the $NF(a^1\Delta)$ - BiF energy transfer process. Another exciting development during this period has been the observation[3] of efficient energy transfer from $NCl(a^1\Delta)$ to iodine atoms, producing excited $I(5^2P_{1/2})$. This process offers an interesting alternative to the two phase chemistry required for conventional oxygen-iodine laser systems ("COIL" devices). Recently, Yang and co-workers have demonstrated gain on the $I(^2P_{1/2})$ - $I(^2P_{3/2})$ transition pumped by this energy transfer process.[4] Apart from these applications, excited singlet nitrenes have drawn significant interest from the basic science community, since these species are isoelectronic to the well studied group VI diatomics. The spectroscopy, reactions, and energy transfer processes of these species offer interesting comparisons and insights into the role of angular momentum correlations in theoretically tractable systems.

This program has involved a broadly based investigation of reactions and energy transfer processes involving excited nitrenes. In particular, we have been interested in methods for producing higher densities of these excited species, in order that we might observe second order processes occurring among the metastables. We have made use of both

pulsed laser photolysis and high velocity discharge - flow methods in this effort. A second objective has been measurement of the rate constants of reactions and energy transfer processes which are key to potential laser systems such as those noted above, in order that these systems might be more effectively modeled.

These objectives were incorporated into three tasks. The first task involved the generation of high densities of $NCl(a^1\Delta)$ via the pulsed photolysis of ClN_3 and observation of the subsequent energy transfer to iodine atoms, within an optical cavity suitable for lasing on the $I(^2P_{1/2})$ - $I(^2P_{3/2})$ transition. A second task involved the assembly of a cooled continuous transverse flow reactor, and efforts to density scale the production of excited $NCl(a^1\Delta)$ by the $H + NCl_3$ reaction. A third task has involved the measurement of rate constants as noted above, and the building of a kinetic model for the $NCl(a^1\Delta)$ - I system.

As will be described below, we have made very good progress on all of these tasks. The overall effort is not yet complete, however, and continues under the auspices of a supplemental SDIO/AFOSR program ("Energy Transfer from Excited Nitrenes at High Densities", AFOSR grant number F49620-93-1-0187) which will continue through May, 1994. This report, then, presents significant but interim results whose final interpretation may be affected by additional data to be obtained in the coming months.

SUMMARY OF RESULTS

Task I. Photochemical Generation of $NCl(a^1\Delta)$

In these experiments, $NCl(a^1\Delta)$ was generated by the photolysis of ClN_3 with the 193 nm output of a pulsed ArF excimer laser. Coombe and Van Benthem[5] have shown that this photolysis produces $NCl(a^1\Delta)$, and minor amounts of excited $N_2(B^3\pi_g)$. Energy transfer to iodine atoms was effected by photolysis of ClN_3/CH_2I_2/diluent mixtures at 193 nm. Pence, Baughcum, and Leone[6] have shown that photolysis of CH_2I_2 at this wavelength produces iodine atoms, of which only 5% are in the excited $5^2P_{1/2}$ state. Hence, upon photolysis of the ClN_3/CH_2I_2/diluent mixture, $NCl(a^1\Delta)$, $I(^2P_{1/2})$, and $I(^2P_{3/2})$ are created simultaneously and the subsequent loss of excited NCl and production of excited $I(^2P_{1/2})$ is readily observed. Ray and Coombe[7] have used this method to measure the rate constant of the energy transfer process, and Figure 1 shows data from their experiments. Figure 1a shows the decay of $I(^2P_{1/2}) \rightarrow I(^2P_{3/2})$ emission at 1.315 μm following photolysis of CH_2I_2/diluent alone. Figures 1b, 1c, and 1d show similar emission from photolysis of ClN_3/CH_2I_2/diluent mixtures, at different fluences of the 193 nm photolysis laser. The growth of the $I(^2P_{1/2})$ signal (hereafter I*) is clearly evident, and the enhancement of the I* signal by the presence of ClN_3 increases with increasing fluence.

In the present experiments, we have used this method in an effort to generate densities of $NCl(a^1\Delta)$ and I* commensurate with lasing or observable gain. A further objective was the observation of possible second order energy pooling or self annihilation processes among the $NCl(a^1\Delta)$ and I* metastables at these higher densities. The method used was photolysis of

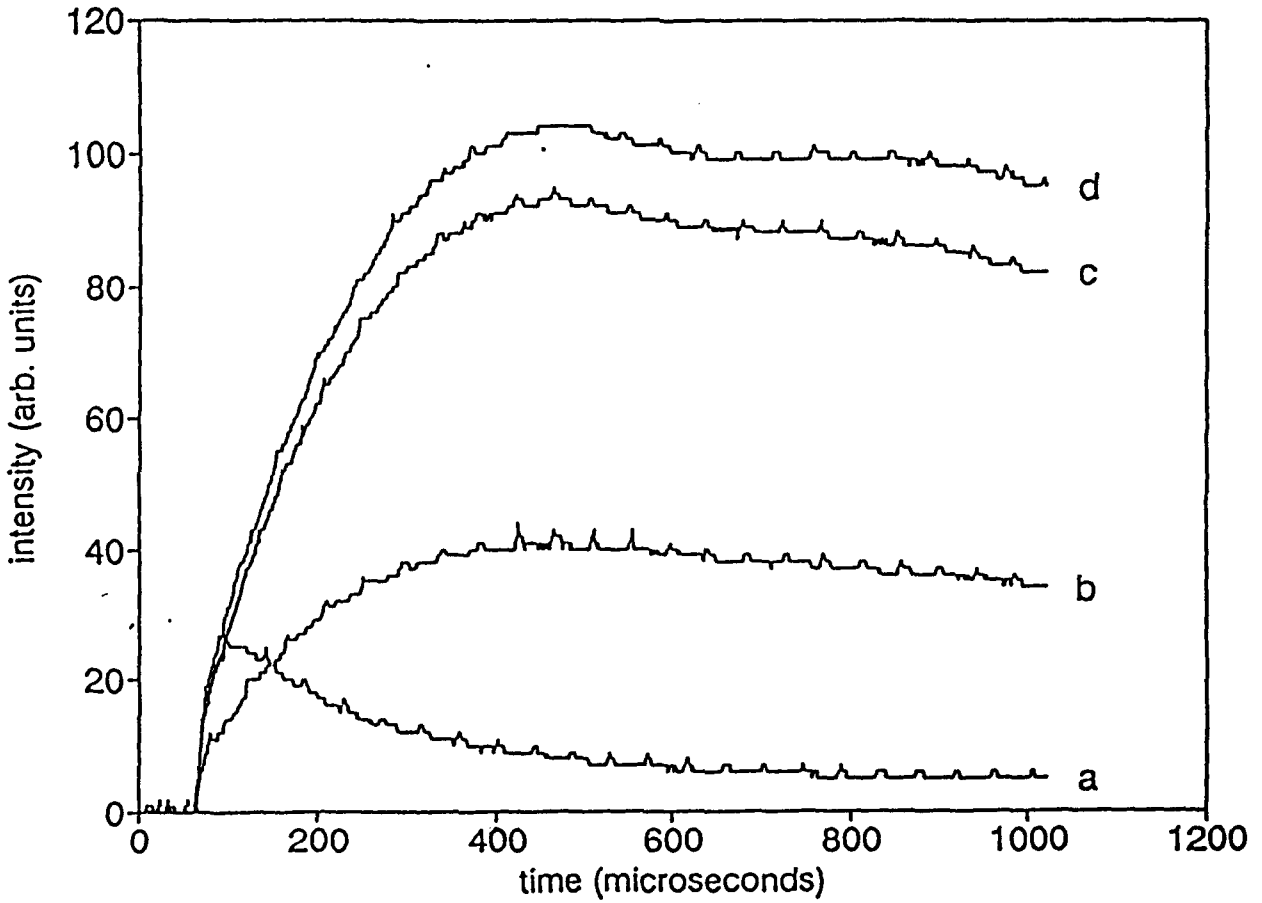

Figure 1. a) Time profile of 1.315 μm emission from 193 nm photolysis of CH_2I_2, at 59 mJ/cm^2. (b,c,d) Time profiles of 1.315 μm emission from photolysis of a CH_2I_2/ClN_3 mixture at 30, 67, and 76 mJ/cm^2, respectively.

ClN_3/CH_2I_2/diluent mixtures at fluences much higher than those used by Ray and Coombe, such that virtually all of the CH_2I_2 and a large fraction of the ClN_3 initially present were dissociated. At the steady state (i.e., near the peak of the I* emission profiles shown in Figure 1), the following equations hold:

$$[I^*] = \frac{k[I][NCl(a)]}{k_Q[Q]} \qquad (1)$$

$$[I^*] / [I] = \frac{k[NCl(a)]}{k_Q[Q]} \qquad (2)$$

The value of k (the energy transfer rate constant) has been determined by Ray and Coombe[7] to be $1.8 \pm 0.3 \times 10^{-11}$ cm^3 s^{-1}. These authors also determined k_Q to be $2.0 \pm 0.3 \times 10^{-11}$ cm^3 s^{-1} for quenching by ClN_3, the dominant process for loss of I*. Inversion of the I*/I populations requires that one third of the iodine atoms present be pumped to the $5^2P_{1/2}$ state. From the data in Figure 1, this was nearly achieved by Ray and Coombe; their data correspond to an excited state proportion of about 25%. From eqn. 2 above, higher [I*]/[I] ratios might be achieved by increasing the [NCl(a)]/[ClN_3] ratio, i.e., by increasing the photolysis fluence. From the values of k and k_Q, about 35% of the ClN_3 must be dissociated to invert the iodine atoms, at the steady state. To lase the system, the absolute magnitude of the gain (i.e., the absolute magnitude of the inversion density) must be such as to overcome the losses of an optical cavity around the medium.

Figure 2 shows a diagram of the apparatus which was assembled to test these ideas. The photolysis cell was fabricated from 7.6 cm x 2.5 cm aluminum channel, and was 1m

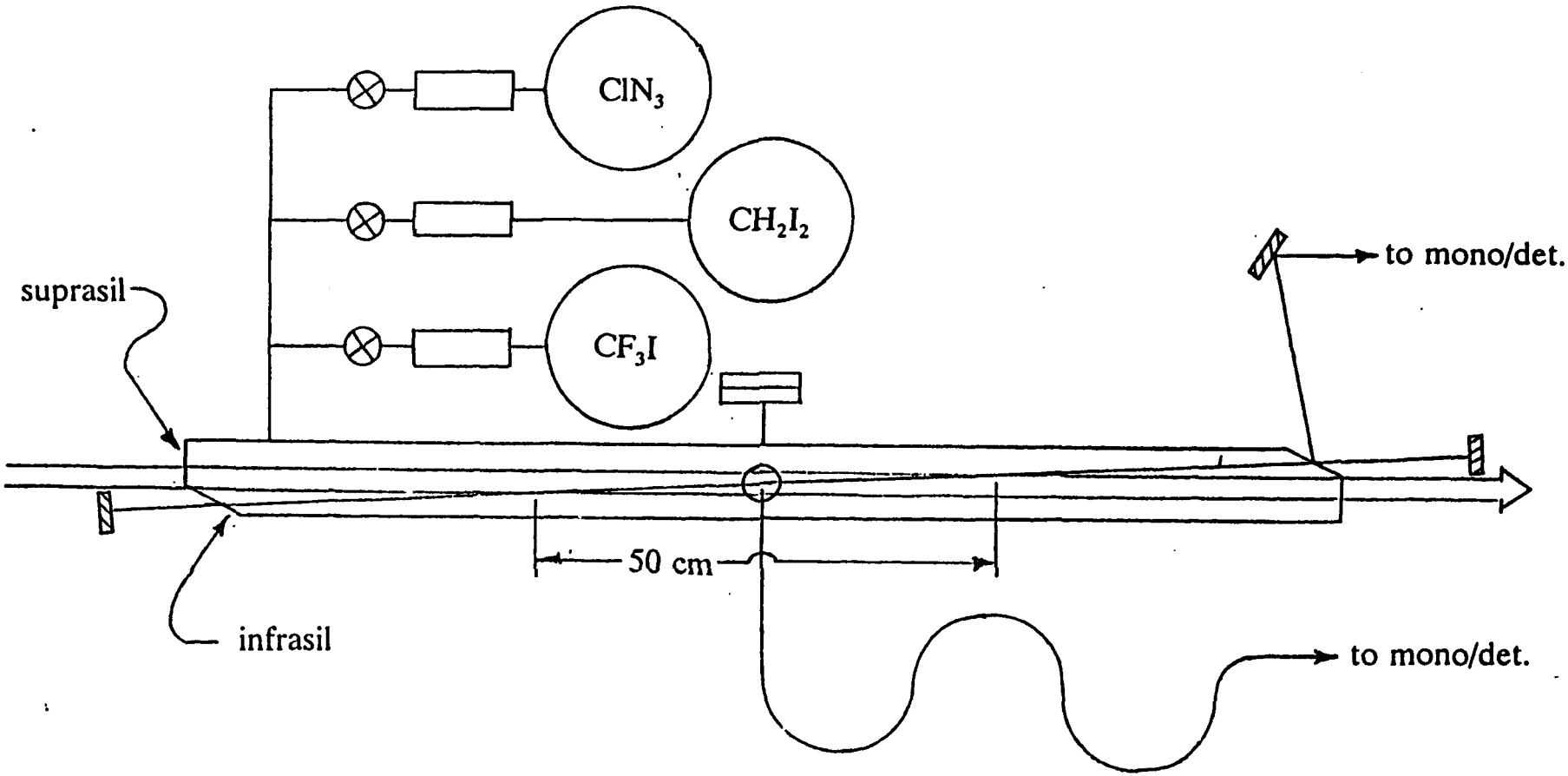

Figure 2. Apparatus used for pulsed I* lasing tests.

long. As shown in the figure, the axes of the photolysis and chemiluminescence/lasing beams were slightly skewed, resulting in a gain length of roughly 50 cm in the system. The windows for transmission of the photolysis beam (193 nm) were suprasil quartz, and those for transmission of the chemiluminescence beam (1.315 μm) were infrasil (both sets from Amersil-Heraeus). The optical cavity for the chemiluminescence beam was comprised of two gold coated mirrors, each with a radius of curvature of 5m. The 1.315 μm emission was taken from the cavity by reflection off the infrasil window near Brewster's angle, as shown in the figure. After transmission to another optical table in the lab, the emission was focused onto the entrance slits of a 0.25m monochromator, which was equipped with a grating blazed at 1.0 μm. After transmission through the monochromator the emission was detected by a cooled intrinsic Ge detector, whose output was recorded on either an oscilloscope or Nicolet 1270 transient digitizer system.

Since the absorption cross section[8] for ClN_3 at 193 nm is 1.38×10^{-18} cm^2 , the saturation fluence at this wavelength is near 0.72 J cm^{-2}. In order to obtain maximum dissociation of the ClN_3, the photolysis laser used was a Questek Impulse excimer laser, capable of delivering more than 0.8 J per pulse at 20 Hz. The cross sectional area of the ArF output beam from this device is near 3 cm^2, such that the maximum fluence for these experiments was about 0.275 J cm^{-2}. This corresponds to a maximum of 58% dissociation of the ClN_3 in the cell, for optically thin conditions.

The sensitivity of the lasing experiment was determined by photolysis of CF_3I in the cell with the 249 nm output of the Questek laser operating on KrF. Photolysis of CF_3I at this wavelength is known[9,10] to produce a 75% yield of I*, and its absorption cross section at 249

nm is well known.[10] Hence the inversion density in the cavity for I* lasing threshold can be determined by observing the CF_3I density and photolysis laser fluence at threshold. The CF_3I for these experiments was obtained from SCM/PCR, and the cell was operated under static fill (i.e., non - flowing) conditions. In practice, lasing threshold was easily observed and was quite sensitve to the CF_3I pressure. Below threshold, the intense I* emission exhibited a rise limited by the time constant of the detector (13 μs) followed by a long decay over several ms. Chemiluminescence observed at the side port of the cell had this same time profile. Above threshold, the detector rapidly saturated (an obvious effect) and stayed that way for several tens of μs, followed by the sub - threshold "tail" over several ms. Very near to threshold, the time profile exhibited a clear "spike" over the sub-threshold chemiluminescence profile. For a photolysis laser fluence of 0.083 J cm^{-2} (measured at the output end of the cell), I* laser threshold was observed for a CF_3I pressure of 150 mTorr. For a CF_3I absorption cross section of 2.60×10^{-19} cm^2, this result corresponds to an inversion density of approximately 1.2×10^{14} cm^{-3}, which in turn corresponds to cavity losses of about 1% per transit.

Samples of gaseous CH_2I_2 were prepared by evaporation from the liquid into 5 liter pyrex bulbs, followed by freeze - thaw cycles at 77K to remove traces of air. The samples were diluted with helium to produce mixtures containing about 0.10 % CH_2I_2. Figure 3 shows the time profile of emission at 1.315 μm observed from the cell containing a density of CH_2I_2 near 1.3×10^{14} cm^{-3}. The I* emission (corresponding to the 5% photolysis quantum yield) is readily visible, and decays over several ms. Samples of ClN_3 diluted in helium (about 2.5% ClN_3) were prepared using methods previously developed in our laboratory,[11]

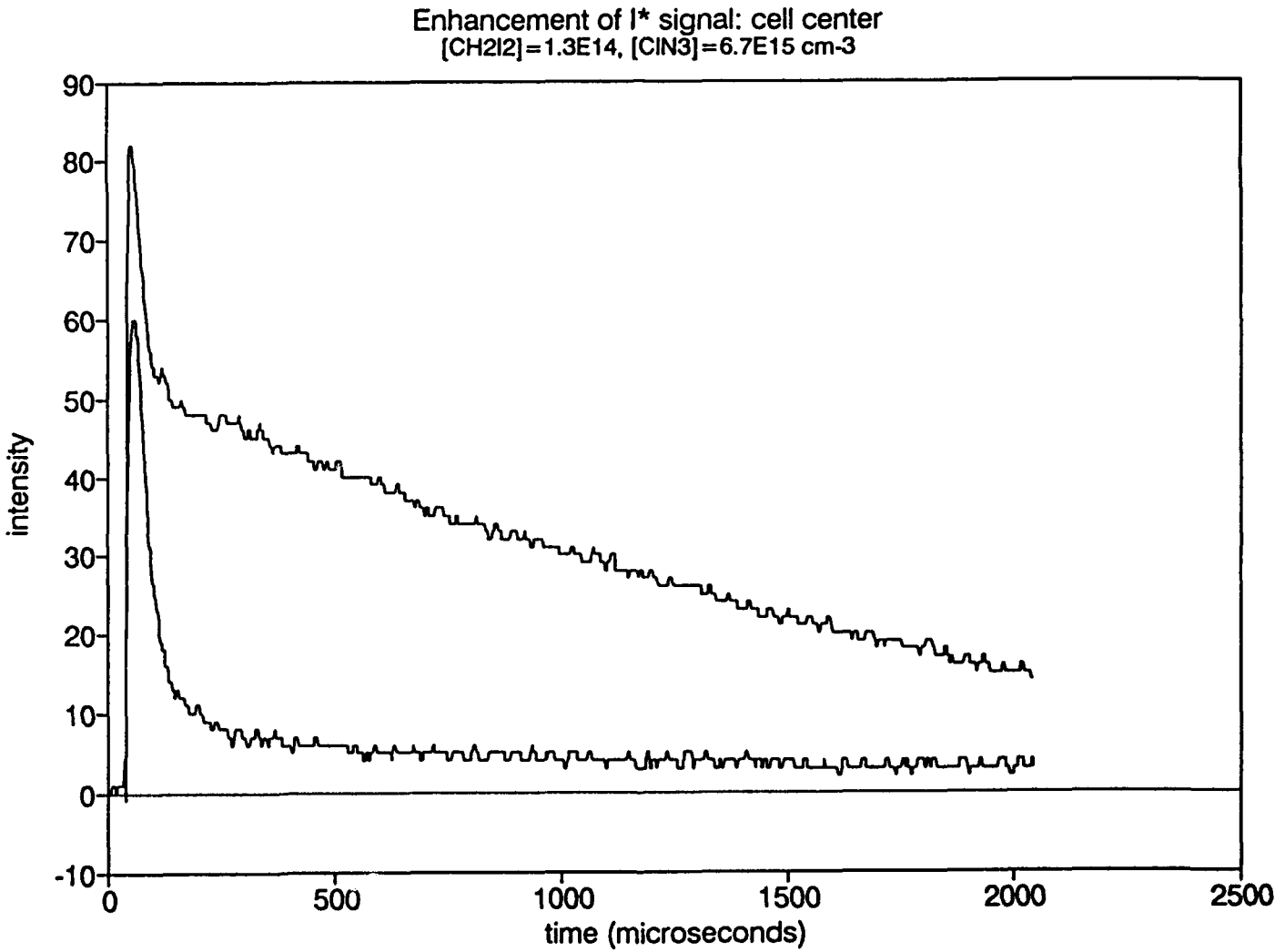

Figure 3. Sample data from the apparatus shown in Figure 2. The lower trace is I* emission from 193 nm photolysis of CH_2I_2/diluent, the upper trace is I* emission from photolysis of CH_2I_2/ClN_3/diluent.

based on passing Cl_2 over NaN_3 suspended on moistened glass wool at 273K. The ClN_3 samples were also contained in 5 liter pyrex bulbs. Photolysis of 6 Torr of the CH_2I_2 mix in combination with 1.5 Torr of this ClN_3 mix resulted in an enhancement of the I* emission intensity by about a factor of 5 over photolysis of the CH_2I_2 mix alone, for a photolysis laser fluence of 0.22 J cm^{-2}. The time profile of the enhanced emission still extended over several ms, and no spiking was observed. For a photolysis laser fluence of 0.27 J cm^{-2} (nearly the maximum for our laser), the enhancement for similar densities was a factor of approximately 7. A sample of these data is also shown in Figure 3. For this enhancement, which implies an I* fractional population of about 35%, the iodine should be slightly inverted but is clearly sub-threshold.

At the maximum densities (ClN_3 at 1.26 x 10^{15} cm^{-3} and CH_2I_2 at 2.0 x 10^{14} cm^{-3}), a substantial fraction of the photons from the photolysis laser are absorbed down the length of the cell. If, for example, nearly all of the CH_2I_2 and about half of the ClN_3 were photodissociated (as expected), about 2 x 10^{17} photons would be absorbed in the 300 cm^3 photolysis volume, or about 25% of all the photons in the photolysis pulse. Hence, the fluence is expected to be much larger near the entrance end of the cell relative to the exit end. From the optical configuration shown in Figure 2 above, the emission monitored off the Brewster window (from the optical cavity) should reflect some average over the length of the cell, weighted toward the intensity at the exit end. The enhancement of the I* emission might well be much larger at the entrance end of the cell relative to the exit end. To probe this possibility, the I* emission was observed at three points in the cavity, using a glass optical fiber which connected the entrance slit of the monochromator to either the entrance

window of the cell, the center port, or the exit window. Indeed, significant differences were found. For photolysis of 8 Torr of the CH_2I_2 mix and 3 Torr of the ClN_3 mix, the enhancement of the I* signal by the presence of ClN_3 in the mix was largest (about a factor of 8) near the entrance window and smallest (about a factor of 3) near the exit window. Further, the emission collected near the entrance window could be increased by increasing the flow of ClN_3, i.e., such that a still larger proportion of the photolysis light was absorbed near the front of the cell. This behavior clearly indicates that the experiment is limited by the fluence of the photolysis pulse; i.e., the medium is simply not optically thin for near threshold conditions. As noted earlier, the more energetic the photolysis pulse, the greater the initial density of NCl(a) and the less important is quenching by residual ClN_3.

Absorption of the 193 nm radiation is still non - uniform but more "even" for the lower density conditions we used originally, i.e., photolysis of 6 Torr of the CH_2I_2 mix (0.10 %) and 1.5 Torr of the ClN_3 mix (2.6%). For these densities and an initial fluence of 0.27 J cm^{-2} at the entrance window, we can calculate that the initial NCl(a) density will be about 7.3 x 10^{14} cm^{-3} near the entrance window, and about 5.4 x 10^{14} cm^{-3} near the exit window. Virtually all of the CH_2I_2 is photodissociated over the full length of the cell. Using these values, we can calculate the maximum I* enhancement (i.e., the factor by which the presence of NCl(a) increases the I* density relative to that produced from the photolysis of CH_2I_2 alone, at a quantum yield of 5%) by using eqn. 2 above. At the entrance window, the maximum possible enhancement would be a factor of 11, and near the exit window it would be a factor of 8. As noted earlier, we observed a factor of about 7 in the experiments, in good agreement with the calculated maximum if we consider that the emission was taken

from the Brewster window near the exit end of the cell. The implication of this agreement is that no new deleterious factors have become significant at this higher density level. Such factors might include NCl(a) self annihilation processes, or I* quenching by species other than residual ClN_3. Were such processes important at these densities (i.e., [NCl(a)] about 7×10^{14} cm^{-3} and [I*] about 1×10^{14} cm^{-3}), the system should be significantly less efficient than the calculated maximum performance.

These calculations suggest that the I* density in the experiments should be on the order of 1×10^{14} cm^{-3}, comparable to that produced in the calibration experiments with CF_3I described above. From the intensity of the I* emission in the two experiments, this is indeed the case. The intensity of the I* emission from the photolysis of the CH_2I_2/ClN_3/He mix is indeed nearly equal to that from 249 nm photolysis of CF_3I at just sub - threshold conditions. Hence, we seem to be making a sufficient amount of I* to lase the system, but the [I*]/[I] ratio is only partially inverted in the CH_2I_2/ClN_3/He experiments. For a ratio [I*]/[I] = 0.67 (an "enhancement" factor of 8), and a total iodine atom density of 2×10^{14} cm^{-3}, the inversion density would be about 1×10^{13} cm^{-3}, only 10% of that required to reach threshold in our cavity.

In the remaining months of the supplemental program, we intend to try pulsed lasing experiments again, with a number of changes. First, we have shortened the cell in an effort to obtain more uniform distribution of photoproducts down its length. Second, we have obtained much higher reflectivity cavity mirrors, which should reduce the cavity losses substantially from the 1% value in previous experiments. Hopefully, I* lasing threshold should occur at inversion densities much less than 1×10^{14} cm^{-3}. Finally, we intend to try

excitation of I* by NBr(a), produced from photolysis of BrN_3. BrN_3 has an absorption cross section[12] at 193 nm about 4 times larger than that for ClN_3.

Task II. Rates of Energy Transfer Processes

A significant difficulty in dealing with the chemistry of excited halogen nitrenes like $NCl(a^1\Delta)$ and $NBr(a^1\Delta)$ is that virtually no data exists concerning the rates of their reactions with or quenching by collision partners. Prior to our work on this program, only a few isolated measurements had appeared in the literature.[13] This is in strong contrast to the situation for the $a^1\Delta$ states of NF or O_2, for which the rate constants of many such processes have been reported.[14-17] In this task, measurements were made of rate constants for the quenching of $NCl(a^1\Delta, v=0)$ by a number of collision partners. The quenchers selected for initial study were chosen for their importance in the chemistry of $NCl(a^1\Delta)$ generation or in the $NCl(a^1\Delta)$ - I system.

For these experiments, NCl(a) was generated by the pulsed photodissociation of ClN_3 at either 193 nm or 249 nm with an ArF or KrF laser, respectively. The photolysis cell was a pyrex cross equipped with fused silica windows for transmission of the laser beam and detection of the NCl $a \rightarrow X$ emission near 1.08 μm. The experiments were performed under slow flow conditions, with the flow rates of ClN_3/He and the quenching gases monitored with calibrated mass flow meters (Tylan). The total pressure in the cell was monitored with a capacitance manometer (MKS). The incident fluence of the ArF laser varied from 0.035 to 0.092 J cm^{-2} in these experiments. This was sufficient to produce between 7% and 17% dissociation of the ClN_3 in the cell, generating initial $NCl(a^1\Delta)$ densities on the order of

10^{12} cm^{-3}. The 1.08 μm emission from this species was passed through an interference filter with a 10 nm FWHM. In effect, the filter passed emission from only the v=0 vibrational level of the NCl($a^1\Delta$) state. The emission was detected by an intrinsic Ge detector cooled to 77K. The response of this detector was digitized, averaged and stored with a Nicolet 1270 signal processing unit and transferred to a PC for analysis.

Before NCl(a) quenching by added species could be investigated, it was necessary to establish conditions where its interaction with the parent ClN_3 was well understood and constant. This was not a simple task. For ClN_3 photolysis at 249 nm, the NCl(a) decay has a distinctly double exponential time profile, as shown by trace (a) in Figure 4. As described below, we attribute the slow component of the decay (which lasts for many ms) to a chain process carried by thermalized NCl(a, v=0). It is apparent that rotationally/translationally excited NCl (a, v=0) produced by the photolysis does not participate in the chain, as is evidenced by the rapid initial decay in the time profile. The intensity in the long "tail" is increased dramatically by the addition of Ar diluent, as shown in trace (b) of Figure 4. Hence, we feel that there is an initial competition between thermalization of the "hot" NCl (a, v=0) from the photolysis with its quenching in reaction with ClN_3 (probably generating NCl_2). In any event, this complex scenario is not suitable for the measurement of NCl (a, v=0) quenching rates by added species.

For ClN_3 photolysis at 193 nm, the intensity in the "tail" of the NCl (a, v=0) time decay is tiny relative to that for photolysis at 249 nm. This behavior is shown in Figure 4, trace (c). We believe that the excess energy available at 193 nm is such that thermalization of the NCl (a, v=0) no longer competes with reactive quenching by the ClN_3 parent. When

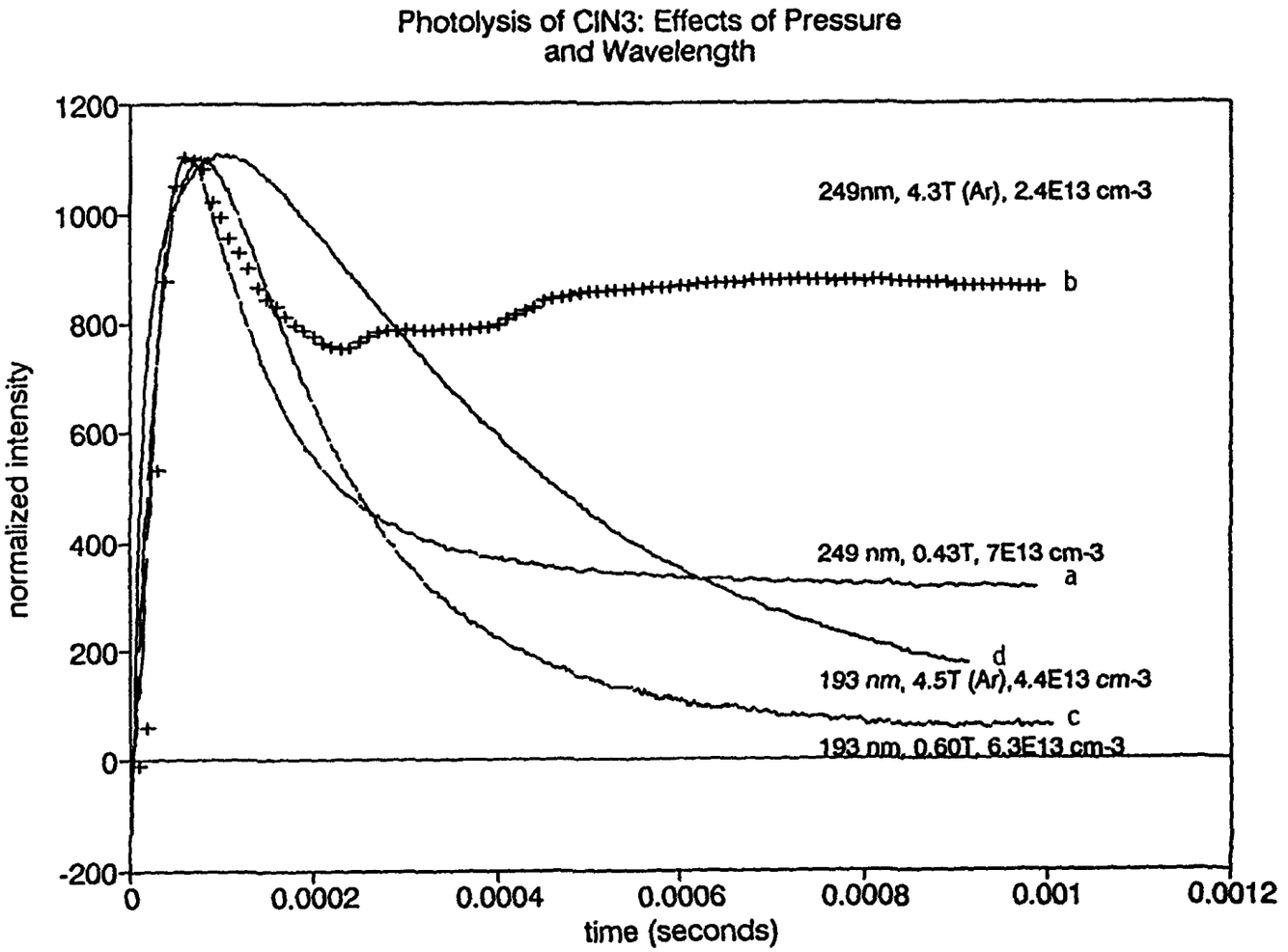

Figure 4. Time profiles of NCl a → X emission from ClN_3 photolysis at 249 nm and 193 nm, with and without added Ar diluent as indicated.

several Torr of diluent is added, the large majority of the time decay is still nicely exponential, as shown in trace (d) of Figure 4. The decay corresponds to the rate of NCl (a, v=0) quenching by ClN_3. Hence, 193 nm photolysis would appear to be the appropriate condition for measurement of NCl (a, v=0) quenching by added species.

The rate measurements were made by recording the exponential decay of the NCl a $\rightarrow$ X emission for fixed ClN_3 and He densities and variable densities of the added quenchers. In this case, the decay rate (λ) is given by

$$\lambda = \lambda_{rad} + \lambda_{diff} + k_{ClN_3}[ClN_3] + k_Q[Q] \qquad (3)$$

Decay by spontaneous emission makes a negligible contribution,[18] as does decay by diffusion for the higher He density as noted above. Hence, for fixed He and ClN_3 densities, the total decay rate varies linearly with the density of the added quencher (Q), and plots of λ vs [Q] are linear with a slope given by the desired rate constant k_Q. Such measurements were made for quenching by seven different diatomics, as well as Ar and He. Plots of k_Q vs. [Q] are shown in Figures 5,6,7, and 8 for these data. Rate constants obtained from the slopes of the plots are collected in Table I, along with literature values for the rate constants of analogous quenching of $NF(a^1\Delta)$ and $O_2(a^1\Delta_g)$.

The rate constants for NCl(a) quenching by the diatomics H_2, D_2, HF, HCl, and DCl show no evidence of the dependence on vibrational frequency or dipole moment indicative[19] of E to V mechanisms, although energy resonances are possible in some cases. There is little or no isotope effect evident in quenching by H_2 and HCl vs. D_2 and DCl. Further, quenching by HF, with its very large dipole, is slower than quenching by HCl. Some other

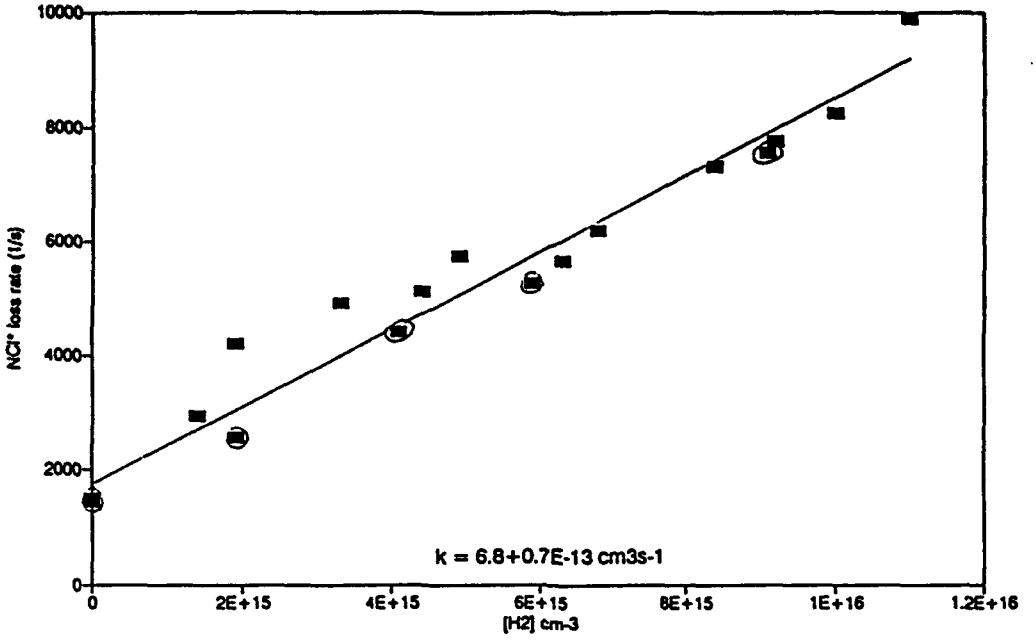

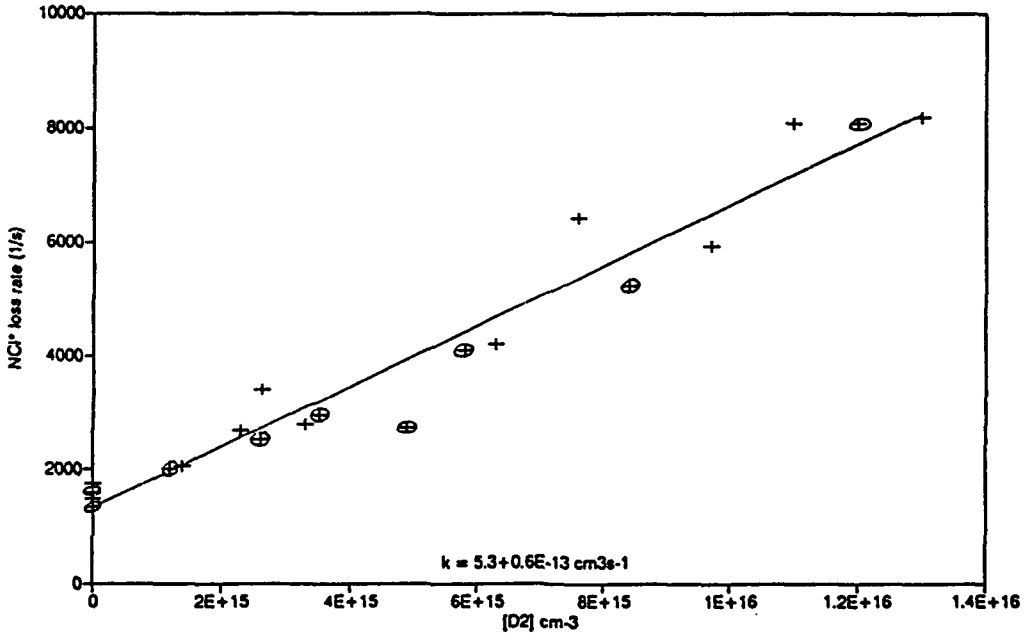

Figure 5. Plots of the exponential decay rates of NCl a → X emission in the presence of H_2 and D_2. Solid lines are least-squares fits to the data.

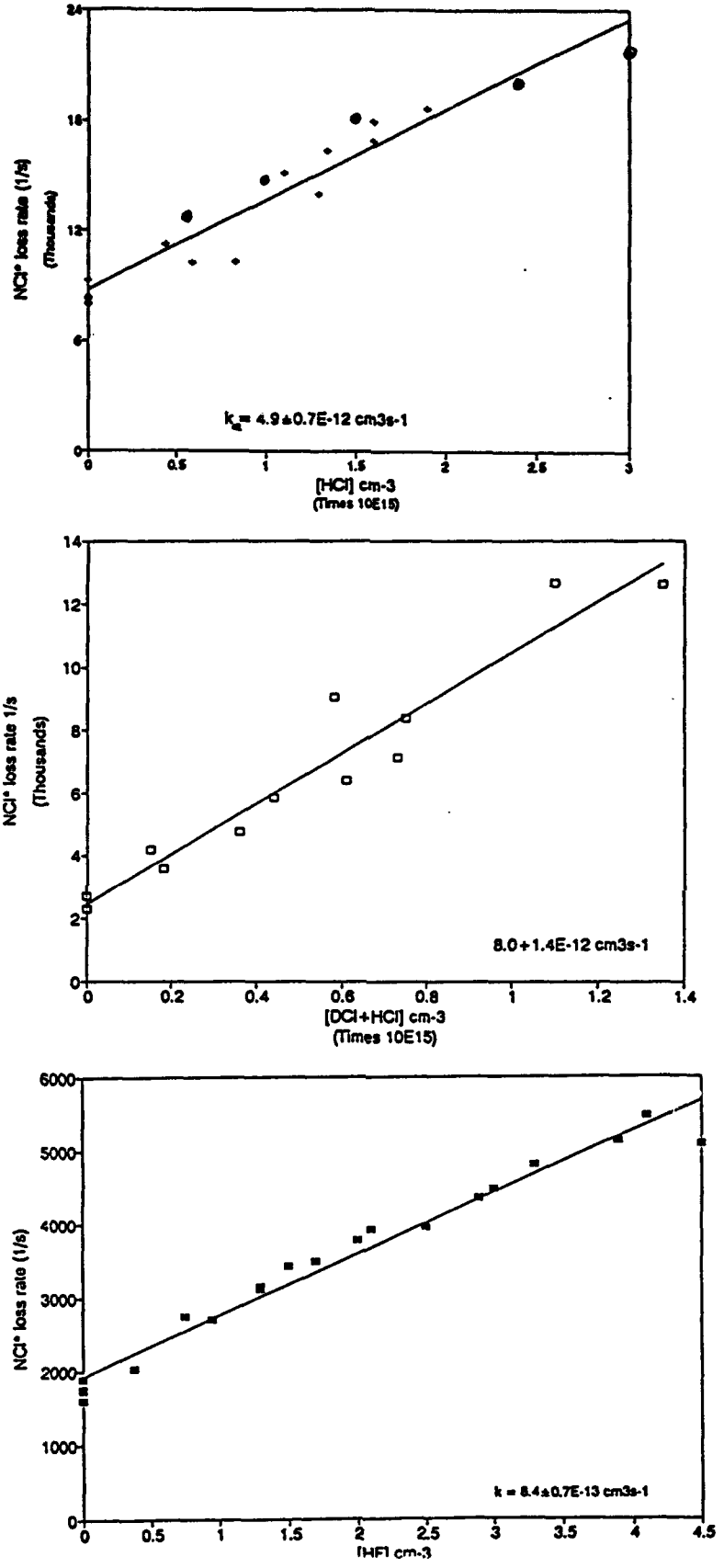

Figure 6. Plots of the exponential decay rates of NCl a → X emission in the presence of HCl, DCl, and HF. Solid lines are least-squares fits to the data.

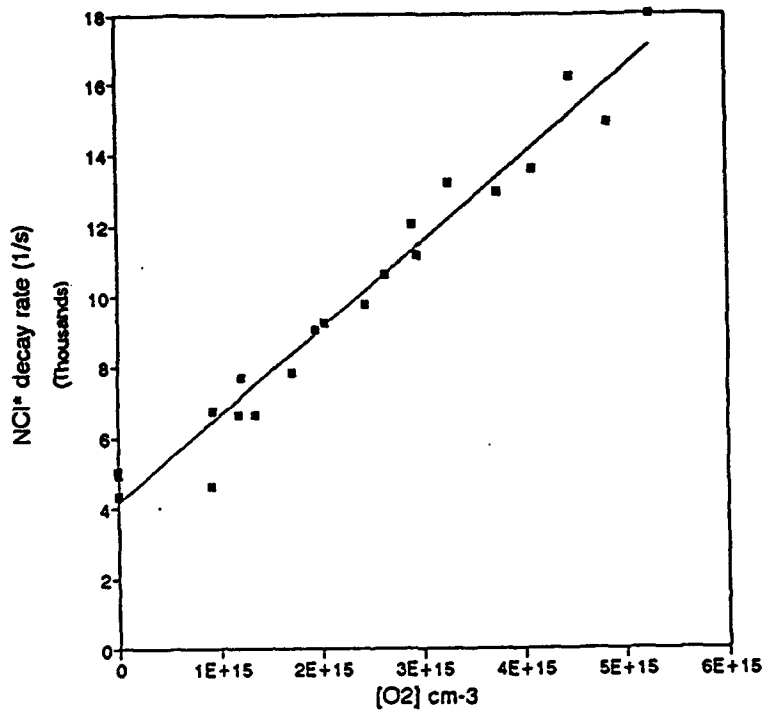

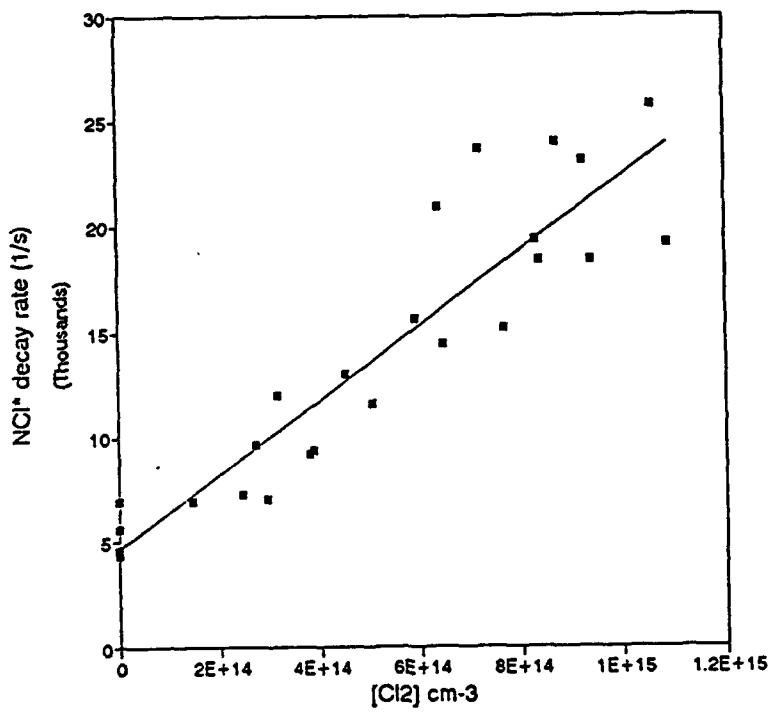

Figure 7. Plots of the exponential decay rates of NCl a → X emission in the presence of O_2 and Cl_2. Solid lines are least-squares fits to the data.

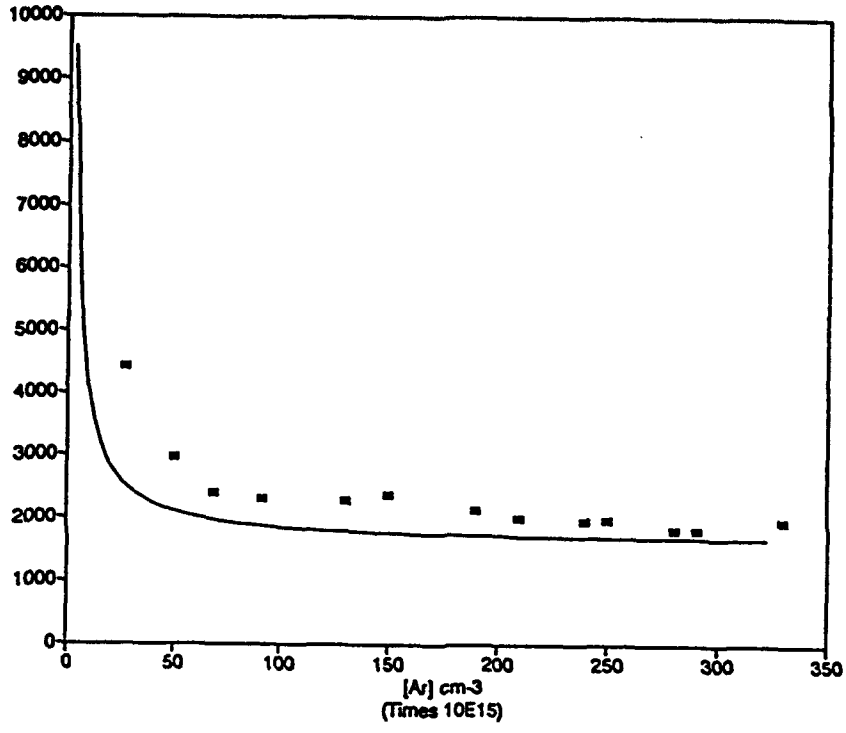

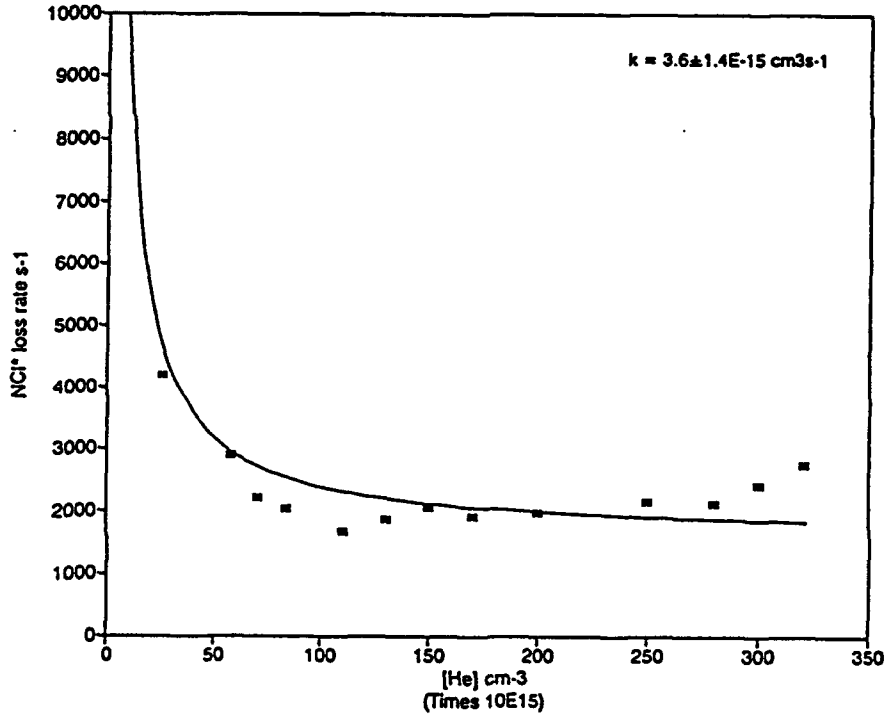

Figure 8. Plots of the exponential decay rates of NCl a → X emission in the presence of Ar and He. The solid lines are the results of a calculation which takes into account diffusion and quenching by the ClN_3 parent.

Table I

Rate Constants for Collisional Quenching of $NCl(a^1\Delta)$

reported in cm^3 $molecule^{-1}$ s^{-1}

	$NCl(a^1\Delta)$[a]	$NF(a^1\Delta)$[b]	$O_2(a^1\Delta)$[c]
O_2	$2.5 \pm 0.2 \times 10^{-12}$	$7.0 \pm 0\ 7 \times 10^{-15}$	$1.8 \pm 0.4 \times 10^{-18}$
Cl_2	$1.8 \pm 0.3 \times 10^{-11}$	$5.8 \pm 0.6 \times 10^{-13}$	$6 \pm 3 \times 10^{-18}$
H_2	$6.8 \pm 0.7 \times 10^{-13}$	$7 \pm 2 \times 10^{-17}$	$4.2 \pm 0.4 \times 10^{-18}$
D_2	$5.2 \pm 0.6 \times 10^{-13}$	-	-
HCl	$4.9 \pm 0.7 \times 10^{-12}$	$1.6 \pm 0.3 \times 10^{-15}$	$4 \pm 3 \times 10^{-18}$
DCl	$8.0 \pm 1.9 \times 10^{-12}$	-	-
HF	$8.2 \pm 1.2 \times 10^{-13}$	3×10^{-15}	$1.4 \pm 0.5 \times 10^{-16}$
Ar	$\lesssim 1 \times 10^{-15}$	-	-
He	$\lesssim 1 \times 10^{-15}$	-	-

[a]The uncertainties listed are 2σ of the least-squares fits to the Stern-Volmer plots.

[b]Refs. 14,15,16.

[c]Ref. 17.

mechanism must be at work. We note in this regard that quenching by Cl_2 is the fastest of the processes measured, suggesting that there may be some correlation between the quenching rate and the stability of the amine-like intermediate in the collision process. For NCl(a) quenching by Cl_2, for example, the collision might well pass through an intermediate configuration similar to an NCl_3 molecule (a stable species). For the other diatomic quenchers measured, such intermediates would be $ClND_2$, $ClNH_2$, HNFCl, $HNCl_2$, and $DNCl_2$, followed by NCl_3 in the order of increasing quenching rate constants. Qualitatively, this is also the order of increasing stability of these amine molecules.[20] This qualitative correlation suggests that short range attractive interactions associated with the bonding potentials of these amines may well be involved in the NCl(a) quenching processes.

The rate constant obtained for NCl(a) quenching by O_2 agrees well with that reported previously by Clyne, Cheah and co-workers[13] (one of the few such numbers in the literature). As suggested by these authors, the mechanism in this case probably involves E to E transfer to generate excited $O_2(a^1\Delta_g)$. Although this process is well off resonance with an exothermicity of nearly 1400 cm^{-1} for generation of O_2(a, v=0), it is much more nearly resonant for generation of O_2(a, v=1), a process which is endothermic by only 87 cm^{-1}. This issue is discussed in more detail below.

NCl(a) quenching by either He or Ar is inefficient, with rate constants in the 10^{-15} cm^{-1} regime. In fact, these values are within the baseline uncertainty limits of our experiments. At lower densities of these rare gases, the dominance of NCl(a) loss by diffusion to the walls is clearly seen (Figure 8). The solid line through the data for Ar is in fact the result of a calculation[21] of the rate of loss by diffusion, given the dimensions of the

cell and assuming unit efficiency for NCl(a) quenching at the wall. The calculation assumed a rate constant for NCl(a) quenching by the ClN_3 or Cl_2 present of 2 x 10^{-11} cm^3 s^{-1} (i.e., the value measured for Cl_2). This constant rate dominates at high Ar densities. The diffusion coefficient used in this model was calculated from the mean free path, with an estimated hard spheres collision cross section for NCl(a). Clearly, the diffusion calculation agrees well with the data.

From Table I, it is clear that in general collisional quenching of NCl(a) is faster than quenching of NF(a) which in turn is faster than quenching of 0_2(a). As above, we expect that this trend reflects in some measure the strength of attractive interactions between these molecules and diatomic quenchers, correlated to the stabilities of intermediate species. We note however, that NF(a) quenching by HCl and NCl(a) quenching by HF may pass through the same amine - like HNFCl intermediate, but the rate constant of the former process is still three orders of magnitude smaller than that of the latter.

For photolysis of higher ClN_3 densities at 249 nm, the NCl(a) decay exhibits the double exponential behavior shown in Figure 4a. The intensity of the long "tail" (which can under some circumstances last for many tens of ms) increases with increasing fluence at fixed [ClN_3], or with increasing [ClN_3] at fixed fluence. In light of the large rate constant reported above for NCl(a) electronic quenching by Cl_2, it is not likely the long tail reflects simple quenching of NCl(a) by the parent ClN_3, but rather some chain mechanism in which the NCl(a) is regenerated. For example, the following process might well occur:

$$NCl(a) + ClN_3 \rightarrow NCl(X) + NCl(a) + N_2 \qquad (4)$$

Here, the fragile ClN_3 is simply dissociated by its collision with NCl(a), which is quenched in the process. Since, however, the ground state of ClN_3 correlates adiabatically to NCl(a) + N_2, the NCl(a) is effectively regenerated in this fragmentation process. Benard and co-workers[22] have shown that this dissociation to NCl(a) occurs thermally, and work in our lab has shown[23] that it can be stimulated by collisions with vibrationally excited species like HF(v). There is every reason to suggest that it would also occur in collisions with electronically excited species like NCl(a). Hence, the long tail in the NCl(a) emission may well reflect the removal of the bulk sample of ClN_3 by a chain carried by the NCl(a) made initially by the photolysis. Increasing the fluence increases the initial amount of NCl(a), such that its steady state density during the chain is greater; hence the larger intensity of the long tail in the decay. Similarly, greater initial ClN_3 densities would result in greater initial NCl(a) densities, and hence greater intensity in the tail, as observed.

A particularly interesting corollary to this chain reaction occurs in the quenching of NCl(a) by 0_2, a process for which the rate constant was reported above. As we noted, this energy transfer process likely generates $0_2(a^1\Delta_g)$. Like NCl(a), 0_2(a) metastables carry sufficient energy to dissociate ClN_3, and a chain carried by both species can be envisioned:

$$ClN_3 + h\nu \rightarrow NCl(a) + N_2 \qquad (5)$$

$$NCl(a) + O_2(X) \rightarrow NCl(X) + O_2(a) \qquad (6)$$

$$O_2(a) + ClN_3 \rightarrow O_2(X) + NCl(a) + N_2 \qquad (7)$$

At the steady state of this chain, both NCl(a) and O_2(a) would be present, in amounts governed by the rates of reactions (6) and (7).

We have obtained evidence of the operation of this chain from experiments in which the NCl(a) - 0_2 energy transfer process is observed at higher initial ClN_3 densities and with 249 nm photolysis. Figure 9 shows the time profiles of the NCl a $\rightarrow$X emission obtained in these experiments, for several different 0_2 densities. Curve 9a shows the NCl(a) time decay in the absence of 0_2; it exhibits the double exponential behavior noted above. Curves 9b - 9e show how the decay profile changes for increasing amounts of 0_2. It is evident that the rate of decay of the long tail does not change appreciably, but its intensity is reduced by increasing amounts of 0_2. In the context of the mechanism above, some of the NCl(a) chain carriers have been converted to 0_2(a), and the 0_2(a):NCl(a) proportion increases with increasing 0_2. We note also that the decay time of the fast component of the time profile shortens with increasing 0_2. This component would be identified with the initial energy transfer process, reaction (6). Indeed, analysis of this decay gives a rate constant in good agreement with that reported in Table I.

This model for the chain mechanism can be used to estimate the rate constant for reaction (7), the dissociation of ClN_3 by $0_2(a^1\Delta_g)$. At the steady state (in the long tail of the NCl(a) decay)

$$\frac{k_6}{k_7} = \frac{[O_2(a)][ClN_3]}{[NCl(a)][O_2(X)]} \qquad (8)$$

where k_6 and k_7 are the rate constants for reactions (6) and (7) above. The value of k_6 is given in Table I. If it is assumed that the decline in the NCl(a) intensity in the tail is caused by conversion to 0_2(a), then the ratio $[0_2(a)]/[NCl(a)]$ can be obtained from the ratio of the

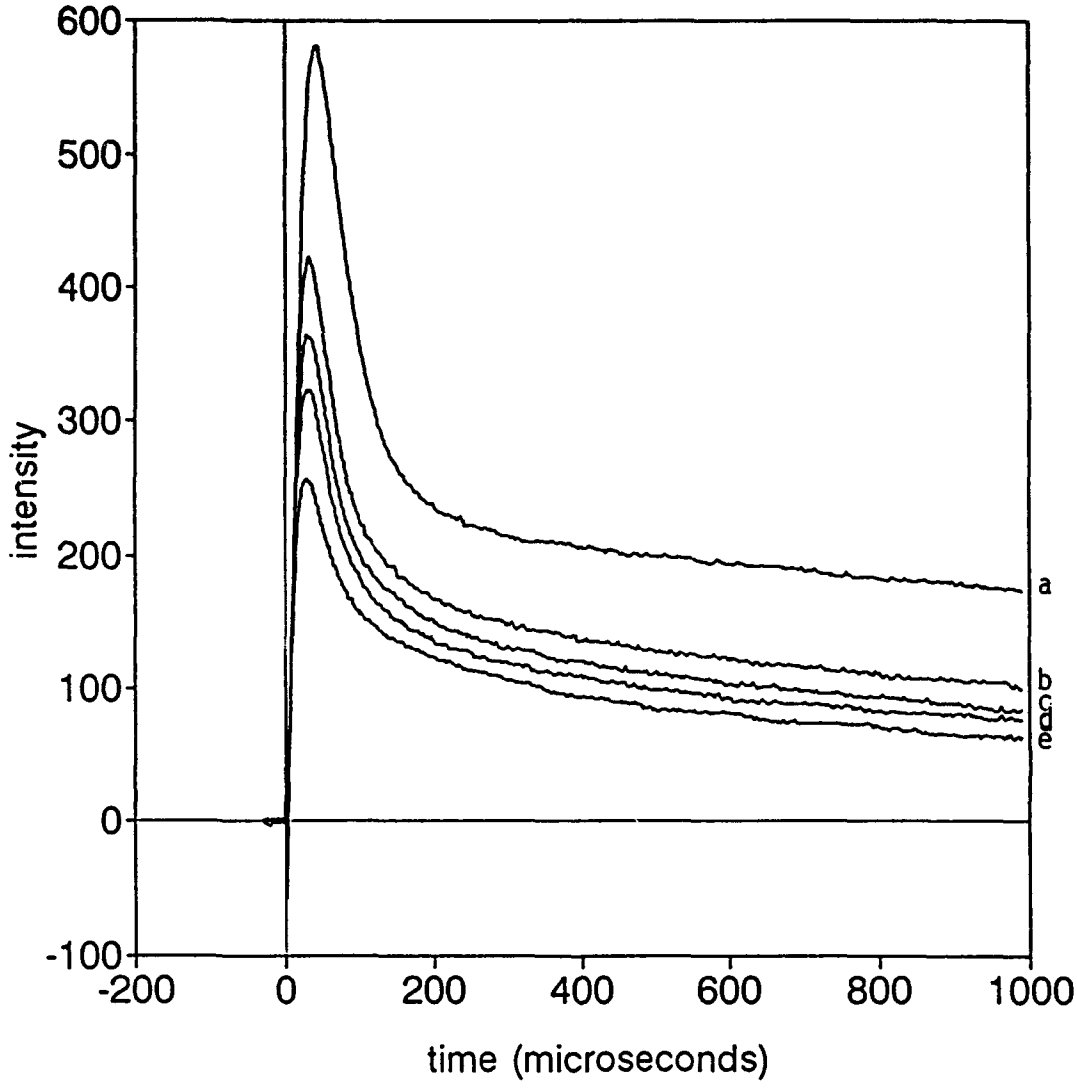

Figure 9. Time profiles of NCl a → X emission produced by 249 nm photolysis of ClN_3 with and without the presence of O_2. a) NCl a → X from photolysis of ClN_3 = 3.8 x 10^{14} cm^{-3} with He = 2 x 10^{16} cm^{-3}, b)-e) photolysis as in (a) but with O_2 = 8 x 10^{14} cm^{-3}, 1.5 x 10^{15} cm^{-3}, 1.9 x 10^{15} cm^{-3}, and 3.8 x 10^{15} cm^{-3}, respectively.

intensity of the tail with and without the presence of 0_2. From this ratio and the measured value of k_6, we can determine k_7. The average value obtained from several such experiments is $k_7 = 1.7 \times 10^{-11}$ cm^3 s^{-1}. The energy transfer process would therefore appear to be quite rapid. Further, the efficiency with which it regenerates NCl(a) must be quite high; from the duration of the tail, many cycles of the chain occur before all of the available ClN_3 is consumed.

These results are important in that they indicate the interchangeability of the NCl(a) and 0_2(a) systems, in the sense that either one might be used to generate the other. For example, Yang and co-workers[24] have reported that NCl($b^1\Sigma^+$), an emitter in the visible, is produced by energy pooling between NCl(a) and I($5^2P_{1/2}$). This system might be accessed by admitting ClN_3 and I_2 to the effluent of a standard BHP-Cl_2 generator[25] for 0_2(a). To test this possibility, we performed a number of experiments in which ClN_3 was admitted to a stream of 0_2(a) generated in a discharge-flow reactor by a microwave discharge through 0_2. An HgO ring was used to remove O atoms from the flow.[26] Such an experiment is expected to perform in a very limited way, since the proportion of 0_2(a) in the 0_2 flow is at best 5% to 10%, and quenching of NCl(a) by ground state 0_2 will dominate over its production by 0_2(a) dissociation of ClN_3. Nonetheless, NCl(a) generation was readily observed upon admission of ClN_3 to the flow. Using a cooled Ge detector and an interference filter for 1.08 μm, the signal was generated when ClN_3 was added and was quenched when the flow was shut off. It would be interesting to perform this experiment with a BHP - Cl_2 reactor, for which the 0_2(a):0_2(X) proportion in the effluent is very much greater.

Task III. Density Scaling the H/D + NCl_3 Reaction

In a previous SDIO/AFOSR supported research program,[27] we showed that the reaction of NCl_3 with H or D atoms is an efficient source of NCl(a) metastables, and that the NCl(a) - I atom energy transfer process can be readily operated by simply adding HI or I_2 to this system. Linear scaling of the system was observed[28] to 10^{13} cm^{-3} densities of both NCl(a) and I*. In this task, a much more sophisticated flow reactor was assembled and tested with the objective of scaling the system to still higher densities.

A diagram of the flow reactor is shown in Figure 10. The mixing head is assembled from water cooled, teflon coated copper blocks. In some experiments the interior surfaces of the reactor were coated with halocarbon wax, as some of the original teflon coating was lost. The mixing head incorporates a 0.5 cm x 4.0 cm flow channel, and has three rows of pinhole injectors, each row with pinholes on both the top and bottom surfaces of the flow channel. Both stainless steel and teflon injectors were used; in each case the pinholes were 0.5 to 1.0 mm in diameter and were spaced by 0.5 cm. Observation ports covered by fused silica windows were positioned 2 cm downstream of the third row of pinhole injectors. The windows were purged by a flow of N_2 during the experiments. The reactor was pumped by a 1500 l min^{-1} mechanical pump. For normal operating conditions (pressures near 1.5 Torr, largely Argon diluent), the linear velocity in the reaction block was near 8000 cm s^{-1} .

Creation of a stable flow of H or D atoms, at densities in excess of 10^{15} cm^{-3}, was the first objective of this task. The reactor was originally designed to operate with a 500 amp, 6kV dc discharge for the creation of atoms at the entrance to the reaction block. Preliminary tests of this discharge indicated that it was very inefficient at generating H atoms,

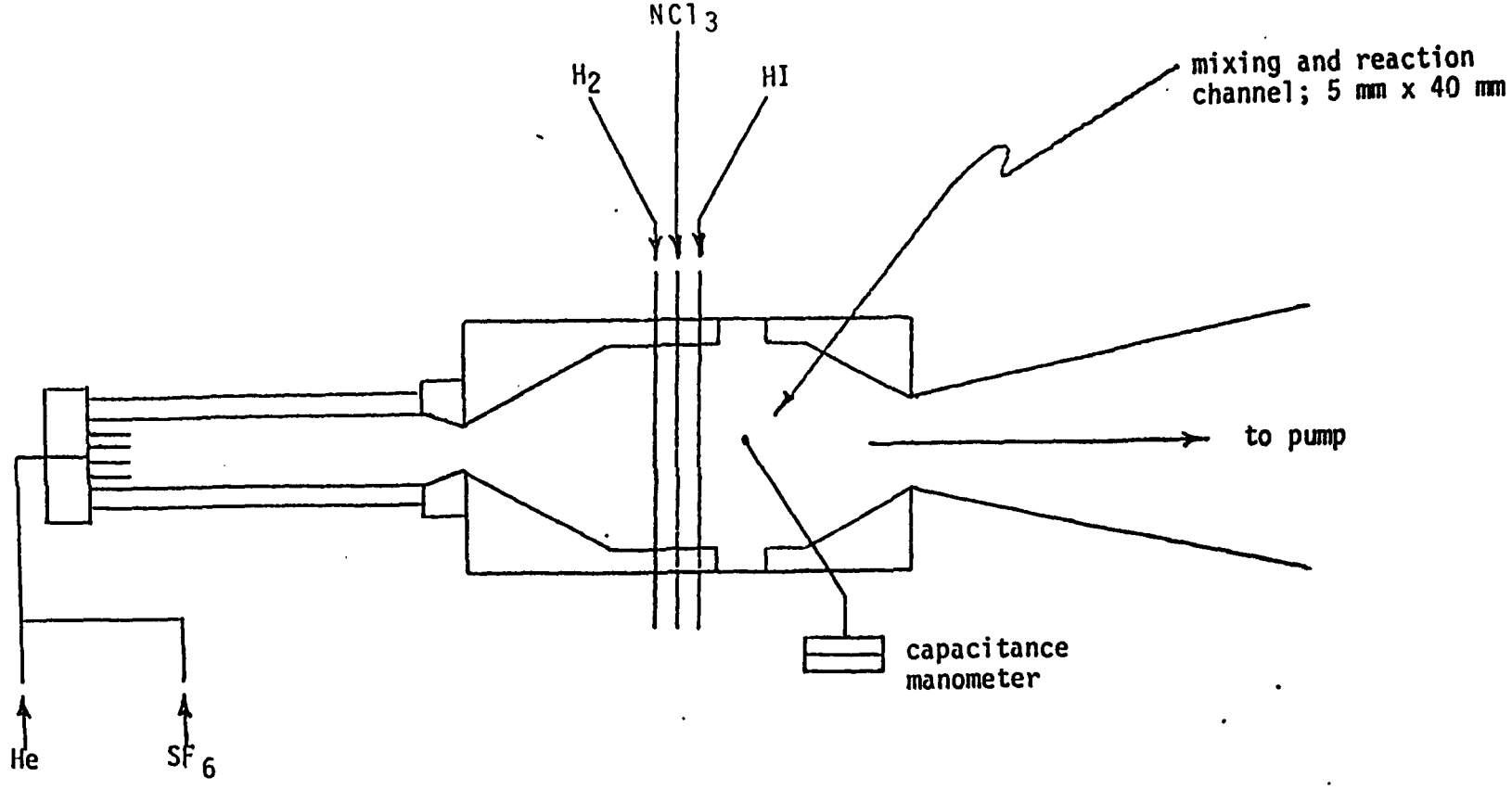

Figure 10. Diagram of the transverse flow reactor, in its original configuration with the dc discharge. Most experiments were performed with a configuration in which the dc discharge was replaced by a dual microwave assembly.

however, and it was replaced by a system of two 100W microwave discharges in parallel. Although H atoms could be generated directly by a discharge through H_2 diluted in Ar, these atoms were rapidly lost by quenching at the reactor walls and the maximum atom density at the observation windows was about 2 x 10^{14} cm^{-3}. The H atoms were titrated by reaction[29] with NO_2, and detected downstream via the HCl(v) infrared chemiluminescence generated by the H + Cl_2 reaction.[30] Variation of the position of the NO_2 inlet relative to the Cl_2 inlet (just upstream of the observation port) showed the rapid loss of the atoms down the reactor. Much better results were obtained by passing an SF_6/Ar mixture through the discharges, then adding H_2 downstream (through the pinhole injectors) to generate H atoms by the F + H_2 reaction.[31] In this case, the atoms were titrated by observation of the infrared emission from HF(v) produced in this reaction. Figure 11 shows a sample of such titration data, as a plot of the intensity of the infrared emission vs. the density of added H_2. The data exhibit a well defined endpoint, which indicates an atom density near 1.5 x 10^{15} cm^{-3}. This is also the density of the HF product, which quenches NCl(a) with a rate constant near 8 x 10^{-13} cm^3 s^{-1} (see Table I). The quenching time for this HF density would be about 830 μs, corresponding to roughly 6.5 cm of flow distance in the reactor. This flow distance is an upper limit, since other quenchers are present as well. Since the NCl_3 is admitted to the system 2 cm (about 250 μs) upstream of the observation port, some quenching by the HF present is expected; for quenching by HF alone at this density, The NCl(a) would be quenched to about 74% of its initial value by the time it reaches the observation zone.

NCl_3 was generated by bubbling Cl_2 through acidified ammonium sulfate, as described previously.[32] The liquid was trapped at 193K, and allowed to warm to room temperature to

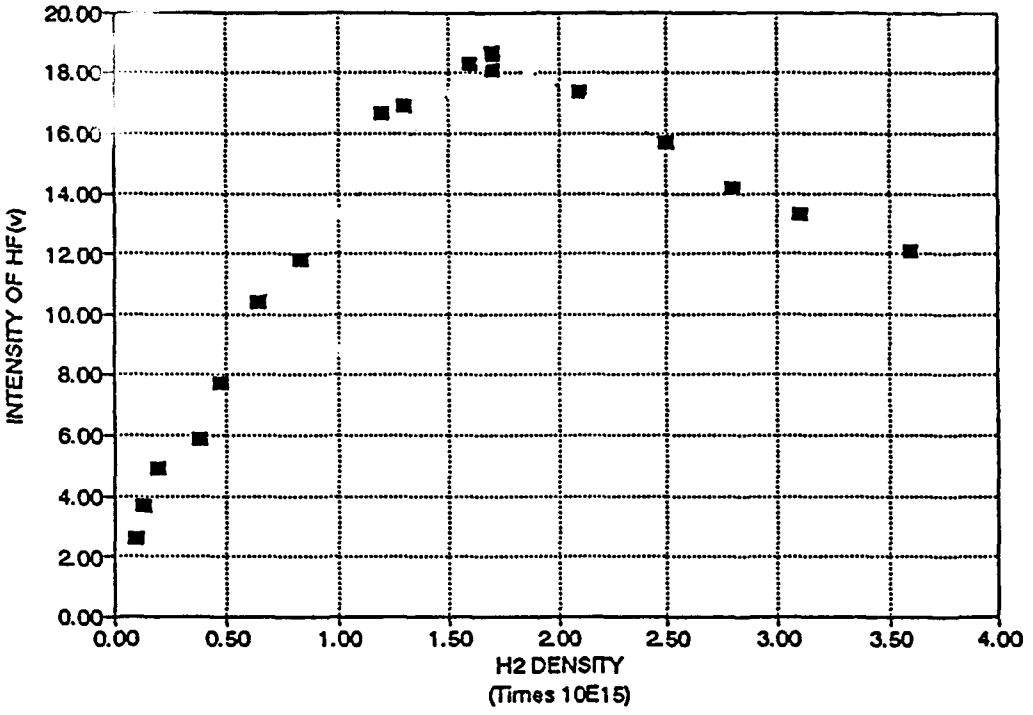

Figure 11. F atom/H atom titration curve, showing the intensity of IR emission from HF(v) vs. the density of added H_2. A clear endpoint is evident at the intensity maximum.

remove any trapped Cl_2. The vapor over the room temperature liquid was entrained in He and flowed into the reactor. Prior to entering the reactor, the NCl_3 proportion in the flow was determined by optical absorption[8] at 253.7 nm as the gas flowed through an 8 mm pyrex absorption cell. The NCl_3 proportion was typically about 6% for our flow conditions. In order to create a more stable NCl_3 flow at higher mass flow rates, the NCl_3 trap (containing the liquid) was substantially enlarged over previous versions, and was equipped with a flat bottom to increase the surface to volume ratio of the liquid. This modification made a significant improvement in our ability to produce controllable flows of this reactive species. The NCl_3/He flow was returned to the fume hood containing the generator, where the total flow rate of the exhaust was measured. The reduction in this exhaust flow rate as the mixture was metered into the reactor was used to determine the flow rate of the NCl_3/He mixture into the reactor. Alternatively, the flow rate was determined by calibrating the pressure rise on admission of the mixture to the reactor. Flow rates corresponding to NCl_3 densities in the reactor greater than 3×10^{14} cm^{-3} (assuming no losses between the metering valve and the reactor) were readily generated with this system.

Admission of the NCl_3/He flow to the stream of H atoms (and HF) produced an easily visible purple - red flame, extending for about 3 cm downstream of the NCl_3 injector. Spectra of this flame were recorded with a glass optical fiber, 0.275 m monochromator, and cooled GaAs photomultiplier tube or cooled Ge detector. The response of the PMT or Ge detector was amplified with a lock-in amplifier (the emission was chopped at the observation window of the flow block) and recorded with a strip chart recorder. Portions of the visible and near IR spectra of this flame are shown in Figure 12. The visible spectrum exhibited

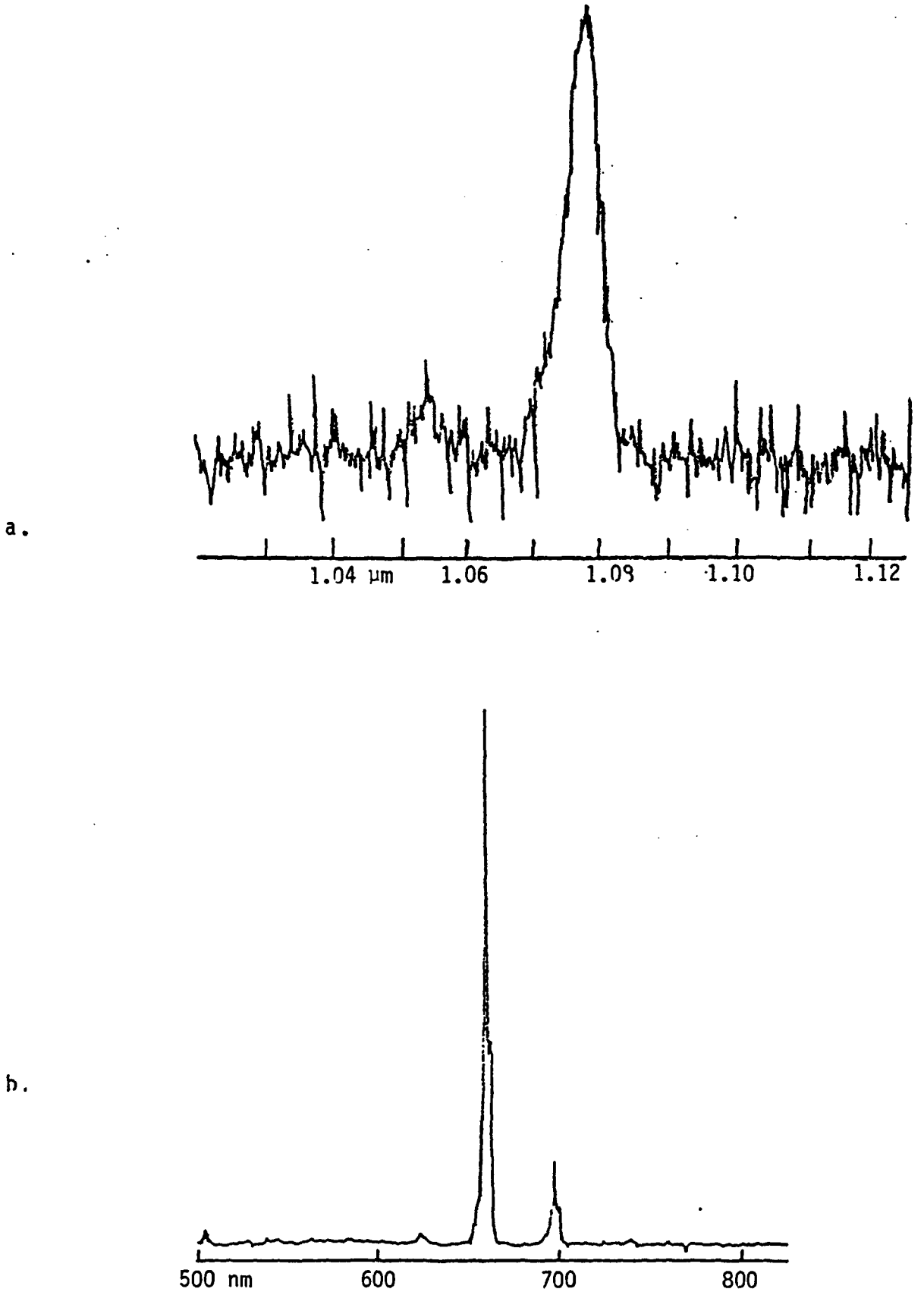

Figure 12. Spectra recorded of chemiluminescence generated in the transverse flow reactor. a) IR spectrum showing NCl a → X emission. b) Visible spectrum showing NCl b → X emission.

weak bands (not shown in the Figure) attributed to the NS $B^2\Sigma \rightarrow X^2\pi$ transition (corresponding to the purple color in the flame). Clearly, some of the NCl_3, NCl_2, or NCl is removed by the products of the discharge through SF_6. The density of excited NS is actually quite small, however, since this species has a 1 μs radiative lifetime.[33] The visible spectrum is dominated by NCl b $\rightarrow$X emission, for which the $\Delta v=0$ sequence lies near 665 nm. Since the lifetime[34] of this emitter is 630 μs, its density exceeds that of the excited NS by more than 3 orders of magnitude. No other emission was observed in the visible region. The only emission evident in the near IR is the NCl a $\rightarrow$X emission. No evidence of excited N_2 was found; the 0,0 band of the N_2 B $\rightarrow$X transition[35] (the first positive emission) should appear near 1.04 μm, and it is clearly absent.

Figure 13 shows a plot of the intensity of the NCl a $\rightarrow$X emission vs. the calculated initial density of NCl_3 in the flow. The plot is clearly curved, the intensity falling off at the higher NCl_3 flows. This is in contrast to results from the previous transverse flow experiments[28] in which linear scaling was observed to NCl(a) densities of 1 x 10^{13} cm^{-3}, produced from initial NCl_3 densities near 1 x 10^{14} cm^{-3}. Originally, we wondered whether the new data might correspond to much higher NCl(a) densities and whether the roll-off observed was a phenomenon of this higher density regime. To test this hypothesis, we determined absolute NCl(a) densities by calibrating the responsivity of the detection system (glass fiber optic, 0.275 m monochromator, and cooled Ge detector) by using the well known O + NO reaction as an actinometer.[36] This method has been employed many times previously in our laboratory.[28,37] From the calibration, it was determined that the maximum NCl a $\rightarrow$X intensities observed in these experiments actually correspond to densities

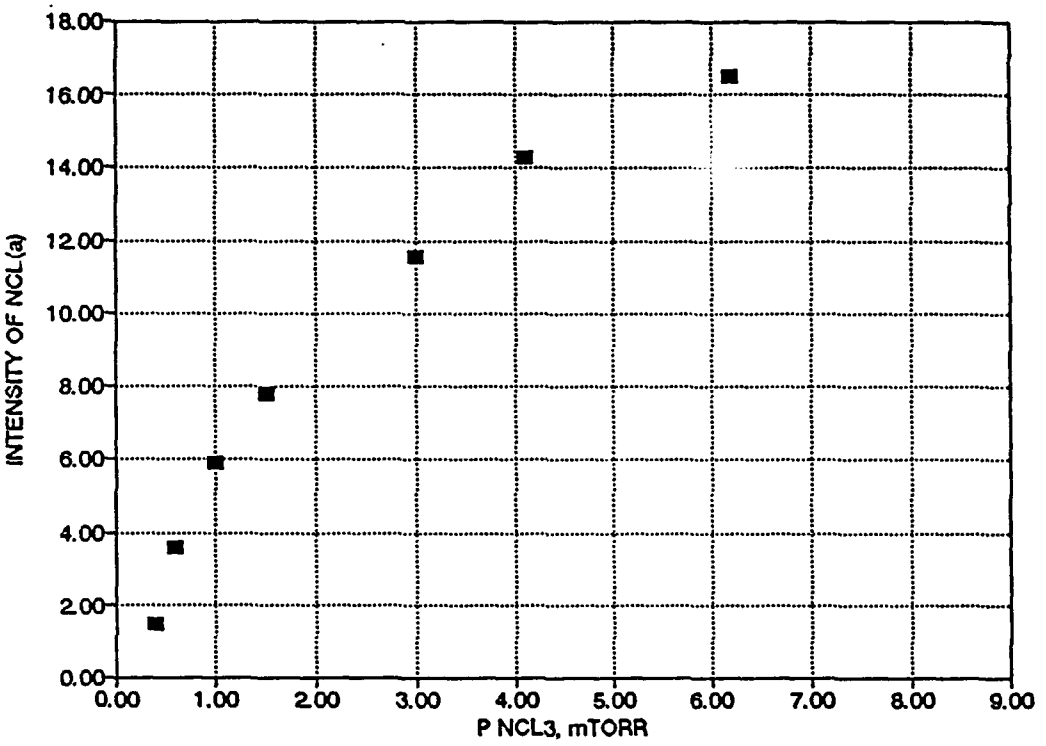

Figure 13. Scaling plot showing the increase of the NCl a → X intensity with increasing NCl_3 density.

somewhat smaller than those previously generated, with a maximum of about 5 x 10^{12} cm^{-3}. It seems clear, then, that the roll-off (and our inability to generate higher densities of excited NCl) must be caused by differences in the chemical environments of the present and previous experiments. The most obvious difference is the use of a discharge through SF_6 to generate F atoms, and H atoms by the subsequent F + H_2 reaction. In the previous experiments, H atoms were generated by a discharge directly through H_2. Although the present method generates HF at densities as large as those of the H atoms, NCl(a) quenching should not be a factor, given the rate constant for this process shown in Table I above. It seems more likely that the NCl_3 reagent is reacting with the SF_6 discharge products, as suggested by the observation of excited NS in the emission spectrum shown in Figure 13. Very recently, we disassembled the reactor to check the integrity of the halocarbon wax-over-teflon walls. A heavy brown deposit was found to permeate the wax and coat the downstream plenum. From previous experience,[38] we believe this deposit to be polythiazyl, an N-S polymer. This observation suggests that indeed a significant fraction of the NCl_3 (or NCl_2, or NCl) is reacted away by the SF_6 discharge products. At present, we are reconfiguring the discharge to run on F_2 diluted in Ar.

These experiments are clearly incomplete, and we intend to continue them during the additional four month duration of the supplemental program described above. At this point, the primary issues still seem to be associated with the generation of an acceptably high flow (and density) of H atoms in a chemical environment which is benign to the NCl_3, NCl_2, and NCl. The F + H_2 reaction seems to be a reasonable way to do this, as we have shown that H atom densities well in excess of 10^{15} cm^{-3} can be generated in our flow reactor using this

reaction, and because the rate constant for NCl(a) quenching by HF is not large. Hopefully, generation of F atoms from F_2 will prove to be the final solution to this issue. A further goal for the next few months will be to add iodine to the system in the hope of generating substantial (10^{14} cm^{-3} or greater) densities of excited I*. We will do this by simply admitting HI to the reaction mixture via one of the sets of pinhole injectors. We will determine the absolute densities of reagents and products and, using known rate constants for the reactions in question and for quenching processes involving species in the mixture, we will assemble a kinetic model for the system. We hope that this model will allow us to predict scalability of the system beyond the densities we are able to generate in our laboratory, and to identify key issues in the use of this system to pump an I* chemical laser.

REFERENCES

1. See for example High Power Gas Lasers, Proceedings of the SPIE, 1225 (1991).

2. D.J. Benard, J. Appl. Phys., 74, 2900 (1993).

3. R.D. Bower and T.T. Yang, Opt. Soc. Am. B, 8, 1583 (1991).

4. T.T. Yang, V.T. Gylys, and R.D. Bower, Opt. Letts., 17, 1803 (1992).

5. R.D. Coombe and M.H. Van Benthem, J. Chem Phys., 81, 2984 (1984).

6. W.H. Pence, S.L. Baughcum, and S.R. Leone, J. Phys. Chem., 85, 3844 (1981).

7. A.J. Ray and R.D. Coombe, J. Phys. Chem., 97, 3475 (1993).

8. T.C. Clark and M.A.A. Clyne, Trans Faraday Soc., 65, 2994 (1969).

9. T. Donohue and J.R. Wiesenfeld, Chem. Phys. Lett., 33, 176 (1975).

10. E. Gerck, J. Chem. Phys., 79, 311 (1983).

11. R.D. Coombe, D. Patel, A.T. Pritt, Jr., and F.J. Wodarczyk, J. Chem. Phys., 75, 2177 (1981).

12. M.A. MacDonald, S.J. David, and R.D. Coombe, J. Chem. Phys., 84, 5513 (1986).

13. M.A.A. Clyne, A.J. MacRobert, J. Brunning, and C.T. Cheah, J. Chem. Soc. Faraday Trans II, 79, 1515 (1983).

14. K.Y. Du and D.W. Setser, J. Phys. Chem., 94, 2425 (1990).

15. K.Y. Du and D.W. Setser, J. Phys. Chem., 96, 2553 (1992).

16. E. Quinones, J. Habdas, and D.W. Setser, J. Phys. Chem., 91, 451 (1987).

17. R.P. Wayne, Singlet O_2, Vol. I (CRC Press, A.A. Fremer, ed., 1985) pg. 81.

18. D. Yarkony, Jr., Chem. Phys., 86, 1642 (1987); A.C. Becker and U. Schurath, Chem. Phys. Lett., 160, 586 (1989).

19. See for example J.J. Ewing, Chem. Phys. Lett., 29, 50 (1974). A.T. Pritt, Jr., and R.D. Coombe, J. Chem. Phys., 65, 2096 (1976).

20. J. Jander and U. Engelhardt, Developments in Inorganic Nitrogen Chemistry (Elsevier, C.B. Coburn, ed.), 2,70 (1973).

21. D. Husain and R.J. Donovan, Adv. Photochem., 8, 1 (1971).

22. D.J. Benard, M.A. Chowdhury, B.K. Winker, T.A. Sedar, and H.H. Michels, J. Phys. Chem., 94, 7507 (1990).

23. N.P. Machara and R.D. Coombe, unpublished data.

24. T.T. Yang and V.T. Gylys, private communication (1993).

25. D.J. Benard, W.E. McDermott, N.R. Pchelkin, and R.R. Bousek, Appl. Phys. Lett., 34, 40 (1979).

26. R.P. Wayne, Advan. Photochem., 7, 311 (1969).

27. SDIO/AFOSR grant no. AFOSR-90-0296.

28. R.W. Schwenz, J.V. Gilbert, and R.D. Coombe, Chem. Phys. Lett., 207, 526 (1993).

29. L.F. Phillips and H.I. Schiff, J. Chem. Phys., 37, 1233 (1962).

30. K.G. Anlauf, D.S. Horne, R.G. MacDonald, J.C. Polanyi, and K.B. Woodall, J. Chem. Phys., 57, 1561 (1972).

31. D.M. Neumark, A.M. Wodke, G.N. Robinson, C.C. Hayden, and Y.T. Lee, J. Chem. Phys., 82, 3045 (1985).

32. J.V. Gilbert, X.-L. Wu, D.H. Stedman, and R.D. Coombe, J. Phys. Chem., 91, 4265 (1987).

33. Y. Matsumi, T. Manukata, and T. Kasuya, J. Phys. Chem., 88, 264 (1984).

34. A.T. Pritt, Jr., D. Patel, and R.D. Coombe, J. Chem. Phys., 75, 5920 (1981).

35. A. Lofthus and P.H. Krupenie, J. Phys. Chem. Ref. Data, 6, 113 (1977).

36. M. Sutoh, Y. Marioka, and M. Nakamura, J. Chem. Phys., 72, 20 (1980); G.A. Woolsey, P.H. Lee, and W.D. Slafer, J. Chem. Phys., 67, 1220 (1977); A. Fontijn, C.B. Meyer, and H.I. Schiff, J. Chem. Phys., 40, 64 (1964).

37. See for example S.J. David and R.D. Coombe, J. Phys. Chem., 89, 5206 (1985).

38. R.L. Green, G.B. Street, and L.J. Suter, Phys. Rev. Lett., 34, 577 (1975).